Purdue University
Purdue e-Pubs

International Compressor Engineering Conference

School of Mechanical Engineering

2012

Elasto-Hydrodynamic Lubrication Effect in Thrust-Slide Bearings of Scroll Compressors

Noriaki Ishii
d10201@oecu.jp

Takuma Tsuji

Tatsuya Oku

Keiko Anami

Takashi Morimoto

Follow this and additional works at: http://docs.lib.purdue.edu/icec

Elasto-Hydrodynamic Lubrication Effect
in Thrust-Slide Bearings of Scroll Compressors

Noriaki ISHII[1], Takuma TSUJI[1], Tatsuya OKU[2], Keiko ANAMI[3], Charles W. Knisely[4]
Kouichi Nokiyama[1], Takashi MORIMOTO[5], Atsushi SAKUDA[5], Kiyoshi SAWAI[6]

[1]Osaka Electro-Communication Univ., Dept. of Mechanical Engineering,Osaka, Japan.
Tel/fax: +81-72-820-4561, E-mail: ishii@isc.osakac.ac.jp
[2]Research and Development Center, Mayekawa MFG. Co., Ltd., Ibaragi, Japan,
Tel: +81-297-48-1364, Tel/fax: +81-284-62-0605, E-mail: tatsuya-oku@mayekawa.co.jp
[3]Ashikaga Institute of Technology, Dept. of Mechanical Engineering,Tochigi, Japan.
E-mail: anami@ashitech.ac.jp
[4]Bucknell Univ., Dept. of Mechanical Engineering, Lewisburg, Pennsylvania, USA.
E-mail: knisely@bucknell.edu
[5]Air-Conditioning and Cold Chain Development Center, Corporate Engineering Division Appliances
Company, Panasonic Corporation, Shiga, Japan.
E-mail: morimoto.takashi@jp.panasonic.com
[6] Dept. of Mechanical Engineering, Hiroshima Institute of Technology, Hiroshima, Japan.
E-mail: sawai@me.it-hiroshima.ac.jp

ABSTRACT

This paper presents the concept of the Elasto-Hydrodynamic Lubrication (EHL) effect for the thrust slide-bearings in scroll compressors, which accounts for the superior lubrication characteristics of these bearings. The thrust plate undergoes elastic deformation due to axial loading, resulting in the formation of a fluid wedge between the orbiting and fixed thrust plates, a region with very high induced oil film pressure which, in turn, accounts for the remarkably good lubrication characteristics of the thrust slide-bearing. Furthermore, the high oil film pressure induces further elastic deformation of the thrust plate, which forms a lubrication pocket with the thrust plate, more effectively increasing the oil film pressure between the sliding surfaces. The formation of the lubrication pocket was confirmed using FEM analysis and lubrication tests on the elastic deformation of the thrust plate. Subsequently a computer simulation flow chart to analyze the elasto-hydrodynamic lubrication of thrust slide-bearing is presented.

1. INTRODUCTION

Remarkably good lubrication characteristics of the thrust slide-bearings in scroll compressors have been found experimentally by Ishii *et al.* [1-3]. They found that the thrust plate undergoes elastic deformation due to axial loading, resulting in the formation of a fluid wedge, defined by the fluid wedge angle between the sliding surfaces. Ishii *et* al. (2008) calculated the wedge angle using a finite element analysis. Oku *et al.* [4-6] and Ishii *et al.* [7] then used the calculated wedge angle in the average Reynolds equation from Patir and Cheng [8,9] along with the solid contact theory from Greenwood and Williamson [10] for the plastic and elastic contacts between the orbiting and fixed thrust plates to analyze the fluid lubrication on rough sliding surfaces. The derived theoretical model permitted the calculation of a very high oil film pressure.

The present study builds on this previous work to identify the magnitude and shape of the elastic deformation of the thrust plate associated with the high oil film pressure. A finite element analysis shows a significant level of elastic deformation, forming a pocket, which effectively increases the oil film pressure between the sliding surfaces. Without the elastic deformation pocket, the oil flow is outward and reduces the formation of high oil pressure; on the other hand, with the pocket, the oil flows inward to enhance the formation of high oil pressure. This is a real Elasto-Hydrodynamic Lubrication (EHL) effect, resulting in the superior lubrication characteristics of thrust slide-bearings in scroll compressors. Subsequently, experiments were undertaken to confirm the formation of the lubrication pocket with the thrust plate. Finally, a flow chart of a computer simulation is presented to numerically analyze the EHL of thrust slide-bearings in scroll compressors.

2. BASIC CONCEPT OF EHL-EFFECT IN THRUST SLIDE-BEARING

Figures 1(a) to (c) show a representative oil-film-pressure distribution calculated for the major specifications,

shown in Table 1. The inner radius r_i was fixed at 37.85 mm and the outer radius r_o at 65.0 mm. The pressure difference Δp on the thrust plate was 0.6 MPa, and the measured friction surface temperature T_f was at about 70°C, for which the oil viscosity μ takes on a value of 0.013 Pa·s. The wedge angle α is fixed at 4.58 mdeg based on FEM analysis of the elastic deformation of the orbiting thrust plate for Δp = 0.6 MPa. The orbiting speed N was 3600 rpm with an orbiting radius of 3.0 mm, resulting in a bearing surface sliding speed V of 1.13 m/s. The surface roughnesses on the fixed and orbiting plates are assumed to have a Gaussian distribution and are characterized by the standard deviation of surface roughness, σ, which was introduced by Oku *et al.* [5], to which the reader is referred for further details. There were 180 lattice divisions in the tangential direction and 30 in the radial direction in the numerical calculations.

A colored 3-dimensional distribution display of the oil film pressure, calculated for the thrust plate loaded with the resultant thrust force of 5043 N, is shown in Figure 1(a). The corresponding oil film thickness was 3.34 μm at its minimum value and had an average value of 4.43 μm.

The maximum pressure distribution along the radial position is shown in Figure 1(b), where the pressure reaches a maximum of 2.53 MPa, decreasing over 200 degrees around the circumferential position, as shown in Figure 1(c).

Such a very high oil film pressure will naturally induce an additional elastic deformation of the thrust plate, thus forming a lubrication pocket, as illustrated in Figure 2(a). This is a real EHL pocket, resulting in an effective formation of high pressure oil film. With this EHL pocket, the oil flow in the fluid wedge drastically changes relative to oil flow without the EHL pocket, as roughly illustrated in Figures 2(b) and 1(d). Figure 1(d) portrays the oil flow without the EHL pocket as the thrust plate moves toward the right. Note that as the thrust plate moves to the right, the oil flow is outwards, away from the movement axis. A high dynamic pressure is induced due to formation of the fluid wedge, but with the leakage of oil from the fluid wedge, the dynamic oil pressure is somewhat attenuated. In contrast, Figure 2(b) portrays the oil flowing into the highest pressure space in the fluid wedge with no leakage of oil from the

Table 1: Major specifications for calculations

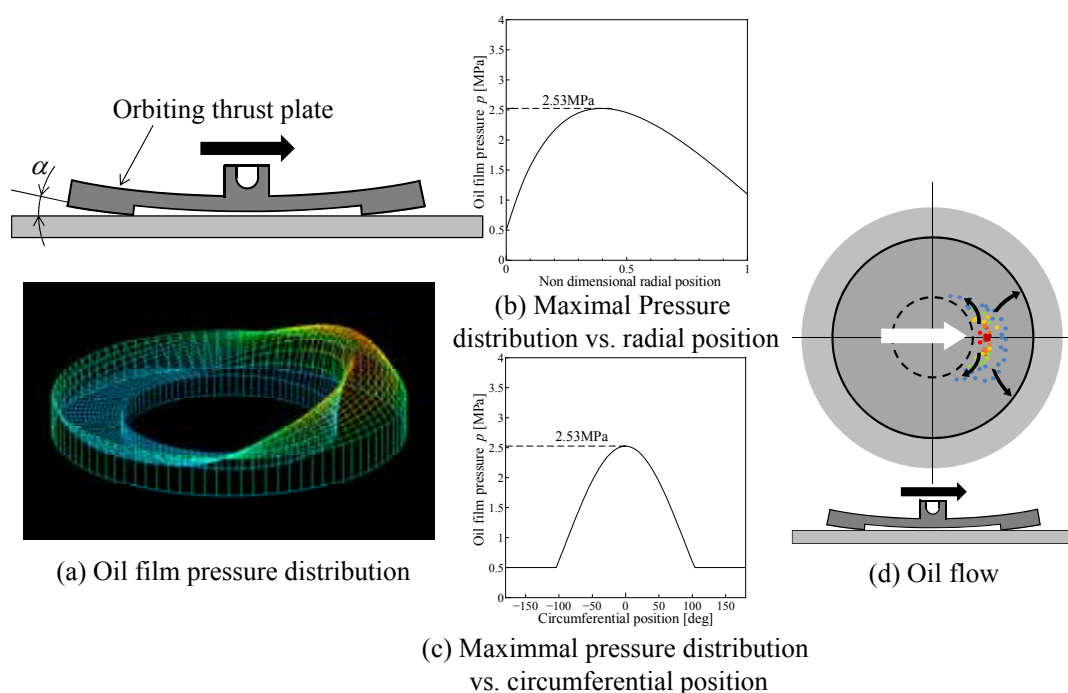|		
Surface roughness Ra	Orbiting thrust plate [μm]	3.0
	Cylindrical thrust plate [μm]	0.056(in) ~ 0.27(out)
Standard deviation of surface roughness	Orbiting thrust plate σ_1 [μm]	1.458
	Cylindrical thrust plate σ_2 [μm]	0.188(in) ~ 1.15(out)
Bearing dimension	Outer radius r_o [mm]	65.0
	Inner radius r_i [mm]	37.85
	Friction surface area S_f [mm^2]	8772.5
Wedge angle α [mdeg]		4.58
Pivot height L_{piv} [mm]		15.0
Cylindrical thrust plate mass m [kg]		0.340
Moment of inertia I_x, I_y [kg m^2]		3.55×10^{-4}
Plastic flow pressure p_c [MPa]		1600
Shearing strength τ [MPa]		240
Surface density of asperities η [mm^{-2}]		400
Asperity summits radius β [μm]		8.0
Oil viscosity μ [Pa s]		0.0069
Tenperature at the surface of thrust plate [ ]		70.0
Inner pressure p_{in} [MPa]		0.5
Outer pressure p_{out} [MPa]		1.1
Pressure difference Δp [MPa]		0.6
Nominal gas thrust force F_p [N]		4443
Spring thrust force F_s [N]		600
Resultant thrust force F_T [N]		5043
Orbiting speed N [rpm]		3600
Orbiting radius r_{obt} [mm]		3.0
Sliding velocity V [m/s]		1.13
Number of grids	Radial	30
	Circumferential	180

(a) Oil film pressure distribution

(b) Maximal Pressure distribution vs. radial position

(c) Maximmal pressure distribution vs. circumferential position

(d) Oil flow

Figure 1: Oil film pressure distribution and expected oil flow, without EHL effect.

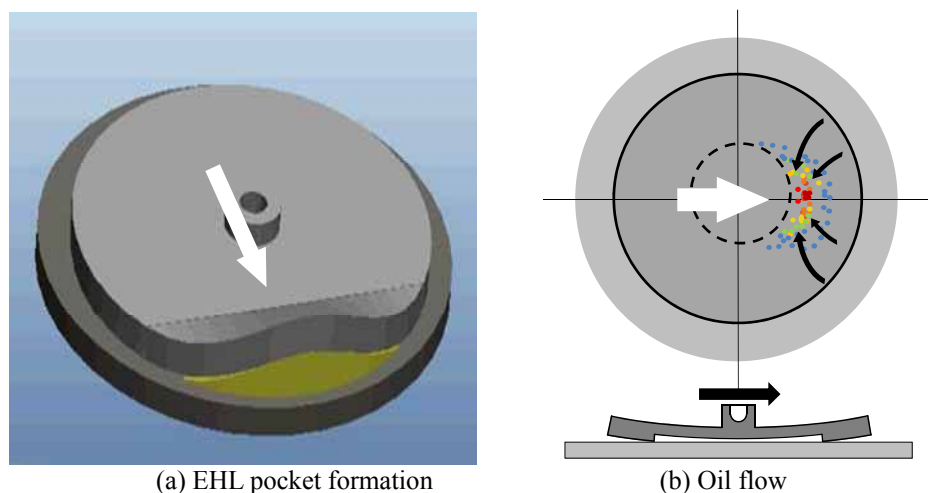(a) EHL pocket formation   (b) Oil flow

Figure 2: Additional elastic deformation of thrust plate due to high oil-film pressure
and resulting oil flow with EHL lubrication pocket.

fluid wedge, thus resulting in a significantly more effective fluid wedge formation at a higher dynamic oil-film pressure. Figure 2(b) portrays the real EHL effect.

3. FEM ANALYSIS AND EXPERIMENTS FOR EHL-POCKET FORMATION

The wedge formation between the friction surfaces can be investigated using FEM analysis for the elastic deformation of the fixed thrust plate. For the FEM analysis, PTC Pro/MECHANICA Wildfire 5.0 software was used on a Dell DIMENSION 8300 PC (CPU: Core2duo, 2.67 GHz× 2, RAM: 3.0 GB, HDD: 450 GB, OS: Windows XP). The thrust plate has a thickness of 10.4 mm, an inner radius of 37.85 mm and an outer of 65 mm, as shown in Figure 3(a). The finite element model of the cylindrical thrust plate, shown in Figure 3(b), was constructed using tetrahedron solid elements. The fixed thrust plate was modeled as a rigid plate element. In the FEM simulations, the pivot bearing port at the center of thrust plate was constrained to permit only movement in the horizontal direction, and a contact condition was imposed between the friction surfaces. In addition, the thrust spring force F_s of 600 N was loaded on the pivot surface and the gas force of 5043 N due to pressure difference Δp of 0.6 MPa was loaded on the thrust plate. Under such loading conditions, the oil film pressure shown in Figures 1(a) to (c) was added to to the load on the friction surface of the thrust plate.

The FEM simulation result is shown in Figure 4.   Figure 4(a) is an elevation view and Figure 4(b) shows the A-A' cross-sectional view. It is quite evident that the EHL pocket is formed with the elastic deformation of thrust plate. The maximum deformation lift at the outer edge of the thrust plate reaches a relatively large value
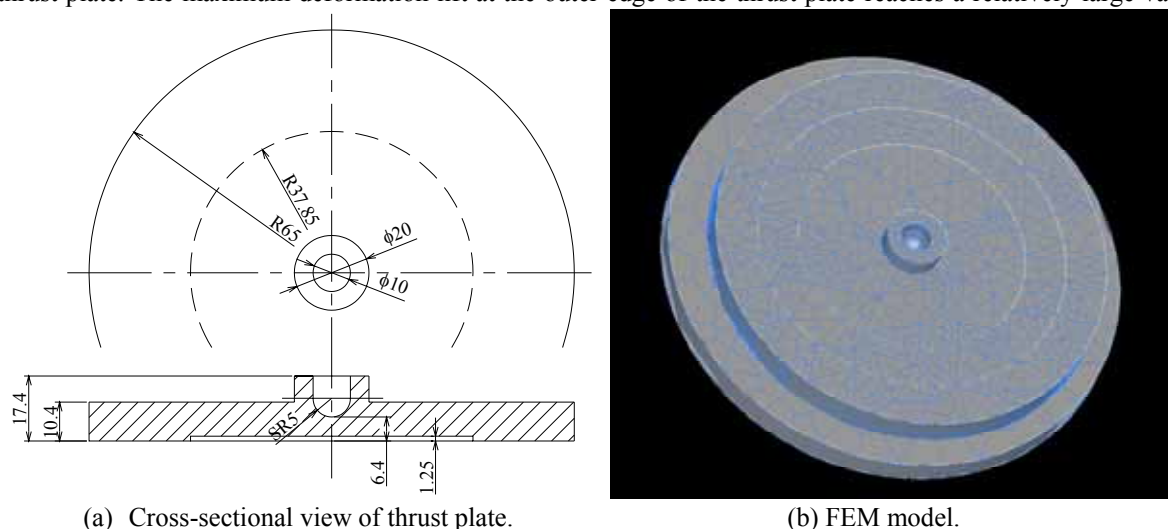
(a) Cross-sectional view of thrust plate.   (b) FEM model.

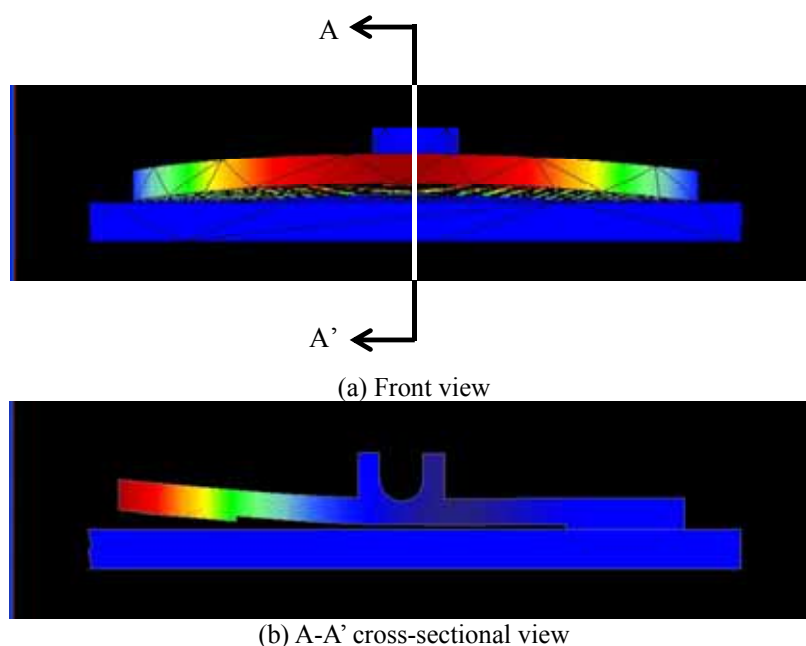Figure 3: Thrust plate and its FEM model

(a) Front view

(b) A-A' cross-sectional view

Figure 4: Deformation of thrust plate simulated by FEM analysis.

of 225 μm. However, this lift is not realistic, because the oil film pressure was assumed to remain constant, independent of the deformation lift. In actuality, the oil film pressure drastically decreases with increasing oil film thickness.   Therefore, the deformation lift cannot be as large as calculated by the FEM analysis. The equilibrium position is a smaller value, just a little larger than the oil film thickness from 3.34 to 4.43μm when calculated using the oil film pressure shown in Figures 1(a) to (c). It is a matter of course that the EHL pocket will also form under these smaller deformations.

In order to confirm the formation of EHL pocket with an actual thrust plate, strain gauges were mounted on the thrust plate with a pitch of 45°, as denoted by positions 1 to 3 in Figure 5(a). Lubrication tests of the instrumented thrust plate were undertaken with a pressure difference of 0.6 MPa and an orbital speed of 3600 rpm. The thrust plate thickness was decreased to 5.0 mm to permit a more easily detected EHL pocket formation The measured strains, shown in Figure 5(b) exhibit fluctuations that synchronize exactly with the orbital speed, and the angle shift of each wave was exactly 45°, indicating the existence of the EHL pocket which rotates at the orbital speed. If there were no EHL pocket, the elastic deformation of thrust plate, induced only by the constant gas and spring forces, would have remained constant and no fluctuation of strain gauge output would have been detected. Therefore, the present experiments clearly demonstrate the existence of EHL pocket as calculated by FEM analysis.

(a) Strain gauges of thrust plate.
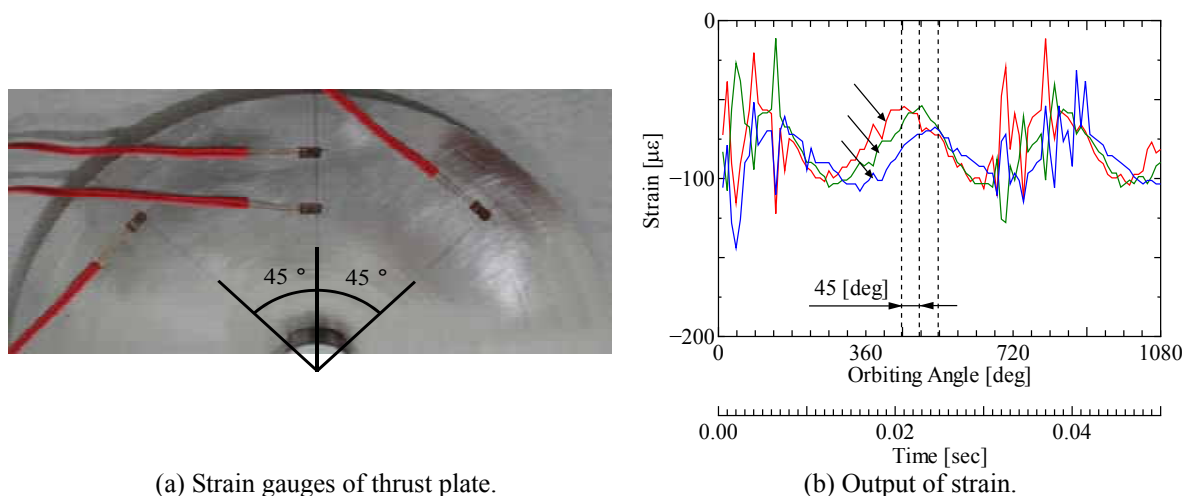

(b) Output of strain.

Figure 5: Measurement of dynamic deformation of thrust plate with pressure difference of 0.6 MPa, operated at orbital speed of 3600 rpm in R-22 environment.

4. SUMMARY OF THEORETICAL ANALYSIS
FOR OIL FILM PRESSURE AND OIL FLOW VELOCITY

Theoretical analysis for lubrication of thrust slide bearing has been developed by Oku *et al.* [5]. A brief summary of the theoretical development is presented here. For more details, the reader is referred to the previous study [5].

For the theoretical calculations of the fluid lubrication by the oil film between the cylindrical and orbiting thrust plates, the wedge formation resulting from the elastic deformation of the cylindrical thrust plate can be mathematically modeled as shown Figure 6. Although, in practice, the wedge angle is thought to result from the elastic deformation of the orbiting plate, the current model is assumed rigid and the wedge angle is simulated by removing a small wedge of material with an included angle of α from the bottom of the outer periphery of the orbiting plate. The cylindrical thrust plate, modified for the purpose of mathematical modeling, has an outer radius r_o and an inner radius r_i. The outer bottom portion of the orbiting plate makes a small angle (*i.e.*, the wedge angle) α at its periphery, as shown in Figure 6. The center of the thrust plate experiences an axial load as represented by the spring force F_s through the pivot bearing. The cylindrical thrust plate can move about the x and y axes, as represented by angular displacements ψ_x and ψ_y, respectively. The x and y axes are the Cartesian coordinates on the orbiting thrust plate surface, with the origin at the center of the cylindrical thrust plate. The corresponding polar coordinates are given as radius r and angle θ.

The oil film is trapped between the fixed and orbiting thrust plates. The boundary pressure on the oil film is indicated by p_{out} at the periphery and by p_{in} at the inner circumference. The boundary velocity on the orbiting thrust plate is indicated by U_1 and W_1 in the x and y directions, respectively:

$$U_1 = V \cos \Theta, \quad W_1 = V \sin \Theta \qquad (1)$$

where V and Θ represent the orbiting velocity and and the orbiting angle, respectively.

4.1 Oil Film Pressure, Thrust and Viscous Forces

With an assumed average clearance height (measured at the center of the orbiting disk) between the cylindrical and orbiting thrust plates, h_o, the oil film thickness h for a case without the EHL pocket is given by the following function in polar coordinates:

$$h(r,\theta) = h_0 + (r - r_i) \tan \alpha - r \cos \theta \cdot \psi_y + r \sin \theta \cdot \psi_x, \text{ where } r_i \leq r \leq r_o \qquad (2)$$

Assuming an isothermal and incompressible oil, the oil pressure p in the elasto-hydrodynamic lubrication between the rough surfaces is governed by the average Reynolds equation relative to the Cartesian coordinates of x and y, derived by Patir and Cheng [8]:

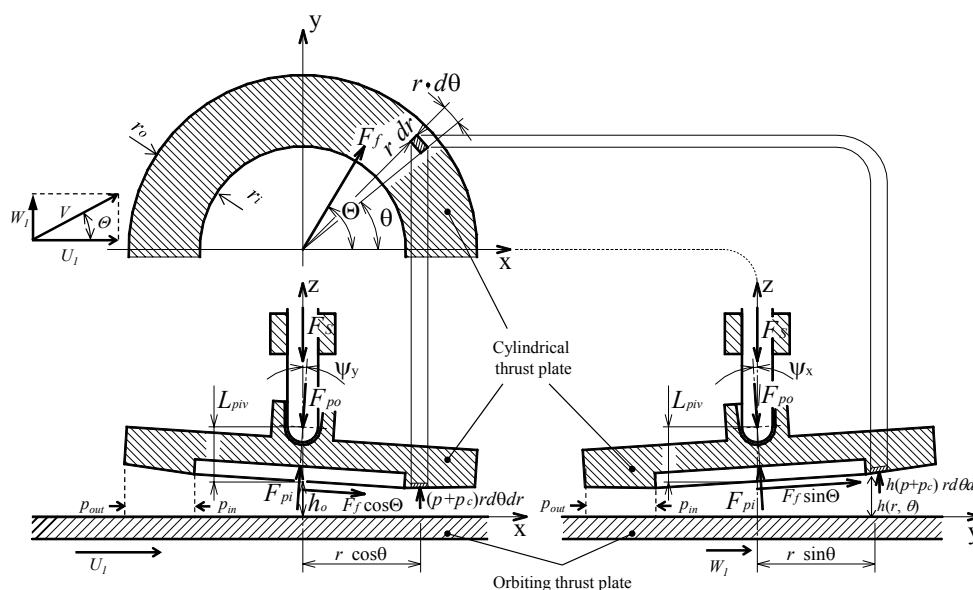Figure 6 Mathematical model of thrust slide-bearing for theoretical analysis of fluid lubrication.

$$\frac{\partial}{\partial x}\left(\phi\frac{h^3}{12\mu^*}\frac{\partial p}{\partial x}\right)+\frac{\partial}{\partial y}\left(\phi\frac{h^3}{12\mu^*}\frac{\partial p}{\partial y}\right)=\frac{U_1}{2}\frac{\partial\bar{h}_T}{\partial x}+\frac{U_1}{2}\sigma\frac{\partial\phi_s}{\partial x}+\frac{W_1}{2}\frac{\partial\bar{h}_T}{\partial y}+\frac{W_1}{2}\sigma\frac{\partial\phi_s}{\partial y}+\frac{\partial\bar{h}_T}{\partial t} \qquad (3)$$

where $\bar{h}_T$ represents the average oil film thickness which can be obtained by integrating the local film thickness h_T. The parameter σ is introduced here to represent the composite rms roughness (i.e., the standard deviation of surface roughness $\sigma=\sqrt{\sigma_1{}^2+\sigma_2{}^2}$); σ_1 is for the orbiting thrust plate and σ_2 is for the fixed plate. The surface roughness can be assumed to have a Gaussian distribution, and hence the average oil film thickness $\bar{h}_T$ is given, depending on the value of H_r, the ratio of oil film thickness to surface roughness. The parameter μ^* in Equation (3) represents the oil viscosity. In addition, the parameter ϕ, the so-called pressure flow factor for isotropic surfaces, represents the effect of surface roughness on the oil flow due to mean pressure difference. ϕ_s, the so-called shear flow factor, represents the effect of the surface roughness on fluid transportation.

In order to apply the average Reynolds equation, Equation (3), to the present axisymmetrical thrust bearing, the Cartesian coordinates (*x, y*) are transformed to the following non-dimensional expression relative to the non-dimensional polar coordinates (*R, θ*):

$$\frac{1}{R}\frac{\partial}{\partial R}\left(\phi RH^3\frac{\partial P}{\partial R}\right)+\frac{1}{R^2}\frac{\partial}{\partial\theta}\left(\phi H^3\frac{\partial P}{\partial\theta}\right)=\lambda\cdot\frac{1}{R}\left\{\frac{\partial}{\partial R}\left(\bar{H}_T\cos(\theta-\Theta)\right)-\frac{\partial}{\partial\theta}\left(\bar{H}_T\sin(\theta-\Theta)\right)\right\}$$
$$+\lambda\sigma\frac{1}{R}\left\{\frac{\partial}{\partial R}\left(\phi_s R\cos(\theta-\Theta)\right)-\frac{\partial}{\partial\theta}\left(\phi_s\sin(\theta-\Theta)\right)\right\}+\sigma_s\frac{\partial\bar{H}_T}{\partial\tau_t} \qquad (4)$$

where the following non-dimensional variables are introduced:

$$R\equiv r/r_o,\;\; P\equiv p/p_a,\;\; H\equiv h/h_{ref},\;\; \bar{H}_T\equiv\bar{h}_T/h_{ref},\;\; \tau_t\equiv\omega t \qquad (5)$$

where the normalizing parameters are the atmospheric pressure p_a, the angular orbiting velocity ω and an arbitrary standard oil film thickness in the thrust bearing, h_{ref}, here taken to be 1μm. The parameters λ and σ_s in Equation (4) are the bearing number determining the bearing load capacity and the squeeze number representing the squeeze film works. Integrating the oil fim pressure $p(r,\theta)$ over the whole bearing surface, the resultant oil film force F_{OIL} can be calculated:

$$F_{OIL}=\iint p(r,\theta)\,rd\theta dr \qquad (6)$$

with the assumption that when the pressure in the bearing surface region becomes lower than the boundary pressure in bearing inner region, p_{in}, it is assigned the value of p_{in}, since the refrigerant in the lubrication oil appears as vapor bubbles in this region. As given by Patir & Cheng [9], the oil film viscous force F_{vs} on the bearing surface with random roughness, due to oil viscosity, can be calculated as

$$F_{vs}=\iint\frac{\mu^*V}{h}\left[\left(\phi_f+\phi_{fs}\right)-2V_{r2}\phi_{fs}\right]rd\theta dr \qquad (7)$$

where ϕ_f and ϕ_{fs} are called "shear stress factors", which represent the effect of surface roughness upon the oil film shearing force (refer to Patir & Cheng [9] for details).

4.2 Solid Contact Force and Its Shearing Force
The solid contact theory by Greenwood & Williamson [10] assumes a plastic contact of a hemispherical projection and a flat plane, to derive the following expression for the local solid contact ratio $\alpha^*(r,\theta)$, defined as the ratio of the local real contact area dA to the local nominal contact area $rd\theta dr$:

$$\alpha^*(r,\theta)\left(\equiv\frac{dA}{rd\theta dr}\right)=\pi\eta\beta\sigma\int_h^\infty(s-h)\phi^*(s)ds \qquad (8)$$

where $\phi^*(s)$ represents a distribution function of bearing surface asperity heights, assuming a Gaussian distribution. η represents the surface density of asperities and β the radius of the asperity summit. Multiplying the plastic flow pressure p_c and shearing strength τ of softer bearing material by the real contact area dA, yields, respectively, the solid contact force F_{sc} and the solid shearing force F_{ss} in the following forms:

$$F_{sc}\left(\equiv\int p_c\cdot dA\right)=\iint p_c\alpha^*(r,\theta)\cdot rd\theta dr \qquad (9)$$

$$F_{ss}\left(\equiv\int\tau\cdot dA\right)=\iint\tau\alpha^*(r,\theta)\cdot rd\theta dr \qquad (10)$$

4.3 Attitude of Cylindrical Thrust Plate

Figure 6 portrays the forces acting on cylindrical thrust plate also, which include the resultant frictional force F_f which is given by the sum of the oil film shearing force F_{vs} and the solid shearing force F_{ss}, the solid contact force F_{sc}, the oil film force F_{OIL}, the spring forces F_s, and the gas forces F_{po} and F_{pi}. The force and moment equilibrium equations are given by

$$-m\ddot{h}_0 + F_{pi} + F_{OIL} + F_{sc} - F_s - F_{po} = 0$$

$$-I_x \ddot{\psi}_x + \iint p(r,\theta) \cdot r \sin\theta \cdot r dr d\theta + \iint \alpha^*(r,\theta) \cdot p_c \cdot r \sin\theta \cdot r dr d\theta - L_{piv} \cdot F_f \sin\Theta = 0$$

$$-I_y \ddot{\psi}_y - \iint p(r,\theta) \cdot r \cos\theta \cdot r dr d\theta - \iint \alpha^*(r,\theta) \cdot p_c \cdot r \cos\theta \cdot r dr d\theta + L_{piv} \cdot F_f \cos\Theta = 0 \qquad (11)$$

where the frictional moment of the pivot bearing is assumed to be negligible, since the pivot radius is comparatively small. The component equations in Equation (11) are all second-order ordinary differential equations with involving the average clearance height (representative clearance) h_0 and the rotation angles ψ_x and ψ_y of the cylindrical thrust plate. The attitude of cylindrical thrust plate is determined so that these differential equations are satisfied.

4.4 Oil Flow Velocity

Non-dimensional oil flow velocity can be calculated in the following expressions:

$$\overline{U} = -\phi \lambda^* \overline{H}_T \left(\cos\theta \frac{\partial P}{\partial R} - \frac{\sin\theta}{R} \frac{\partial P}{\partial\theta} \right) + \frac{\overline{U}_1 \cos\Theta}{2} + \frac{\overline{U}_1 \cos\Theta}{2} \overline{\sigma}\phi_s ,$$

$$\overline{W} = -\phi \lambda^* \overline{H}_T \left(\sin\theta \frac{\partial P}{\partial R} + \frac{\cos\theta}{R} \frac{\partial P}{\partial\theta} \right) + \frac{\overline{W}_1 \cos\Theta}{2} + \frac{\overline{W}_1 \cos\Theta}{2} \overline{\sigma}\phi_s \qquad (12)$$

where the following non-dimensional variables are introduced:

$$\overline{U} \equiv \frac{\overline{u}}{V}, \quad \overline{W} \equiv \frac{\overline{w}}{V}, \quad \lambda^* \equiv \frac{r_o p_{atm}}{12\eta_n V} \left(\frac{h_{ref}}{r_{out}} \right)^2, \quad \overline{\sigma} \equiv \frac{\sigma}{h_T} \qquad (13)$$

4.5 Numerical Calculation Method

The calculation procedure for the case without the EHL pocket, used in the theoretical model of thrust slide-bearing lubrication, is shown by the solid lines in the flow-chart in Figure 7, and ignoring the dashed lines. First, with an assumed attitude for the cylindrial thrust plate (*i.e.*, for assumed values for the average clearance height h_0, and for the rotation angles ψ_x and ψ_y), the clearance height distribution $h(r,\theta)$ is calculated from Equation (2), and the average Reynolds equation, Equation (4), is solved to determine the oil film pressure $p(r,\theta)$. From this pressure distribution, the oil film force F_{OIL} can be calculated using Equation (6) and the oil film viscous force F_{vs} can be determined from Equation (7). In addition, with the solid contact theory, the real contact area is determined from Equation (8), permitting the calculation of the solid contact force F_{sc} from Equation (9) and the solid frictional force F_{ss} from Equation (10). These calculated results are fed back into Equation (11) to determine a more
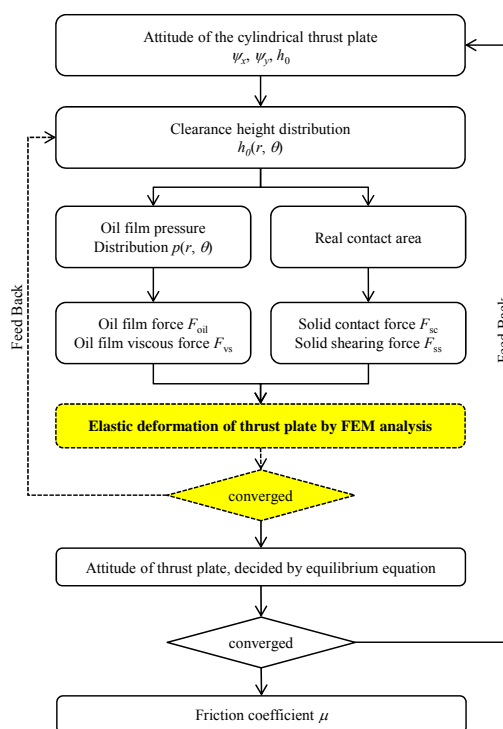

Figure 7: Calculation procedure for lubrication and attitude of thrust-slide bearing, without and with the EHL pocket (dashed lines to be added for the case with the EHL pocket).

(a) Oil film pressure distribution   (b) Average oil flow velocity distribution
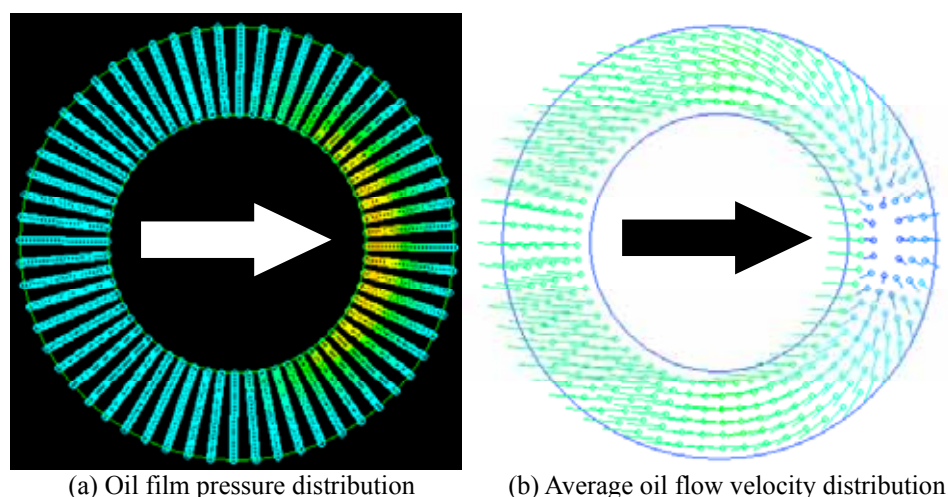
Figure 8: Oil flow velocity by theoretical calculations.

accurate attitude of the cylindrical thrust plate. Finally, after the algorithm converges, the average oil flow velocity is calculated from Equation (12).

For numerical calculations, the Runnge-Kutta method was used to solve Equation (11), where calculations were repeated until a spatially periodic solution corresponding to one revolution of the crankshaft was obtained. Numerical calculation of the average Reynolds equation, Equation (4), required a scheme in which iterative calculations of the difference approximation equation were performed to obtain a converged solution for given boundary conditions. The cylindrical bearing grid consisted of 30 radial and 180 tangential gridlines. The time step in the Runge-Kutta calculation corresponded to 1/60 of one crankshaft revolution period.

4.6 Calculated Results
Oil film pressure calculated for case without the EHL pocket were shown in Figures 1(a) to 1(c). In addition, a colored display of oil pressure is shown in Figure 8(a), where orange represents higher pressure, while blue lower pressure. The oil flow velocity also was calculated, as shown by line vectors in Figure 8(b). These calculated results coincide well with the oil flow, illustrated in Figure 1(d). All oil particles spread outward from the highest pressure space along the movement axis near the inner circle toward the outer region, thus reducing effective formation of high oil film pressure due to fluid wedge.

For the case with the EHL pocket, the dashed lines in the calculation flow chart in Figure 7 must be added to input the shape of EHL pocket, calculated by the FEM analysis, into the whole calculation procedure. Our efforts to determine the oil flow velocity and oil film pressure with EHL pocket have begun, but are not yet complete.

CONCLUSIONS
For quite some time, engineers and other research personnel have noticed that the thrust slide-bearings in scroll compressors experience fewer lubrication issues even though there is no special lubrication pump installed. The thrust slide-bearings instead exhibit high lubrication performance. The reason why the thrust slide-bearing exhibits such excellent lubrication performance was suggested to be due to formation of an oil wedge. The oil wedge forms due to the elastic deformation of the thrust plate, caused by large gas loading on the thrust plate, as documented by experiments and theoretical analysis in references [1-7]. However, the authors had some lingering concerns that the complete explanation of the high lubrication performance of thrust slide-bearings in scroll compressors had not yet been determined. The present paper suggests that the EHL effect occurring in thrust slide-bearings may provide a more complete explanation for the lubrication performance of these bearings. This study presented the basic concept of the EHL effect induced by the EHL pocket. The formation of the EHL was should to be a real possibility using FEM analysis, and was subsequently confirmed with lubrication tests. Subsequently the computer simulation scheme to calculate the excellent lubrication performance due to the EHL effect was presented. However, presently the authors have not yet completed the full EHL analysis, but hope that other engineers and researchers will pay attention to the significance of the EHL effect in scroll compressors.

NOMENCLATURE

dA : Local real contact area, m^2

F_f : Resultant frictional force, N
F_{OIL} : Oil film force, N
F_p : Nominal gas thrust force, N
F_{pi}, F_{po}: Inner gas thrust force, N
F_s : Axial spring force, N
F_{sc} : Solid contact force, N
F_{ss} : Solid shearing force, N
F_{vs} : Oil viscous force, N
h : Nominal oil film thickness, m
h_0 : Average clearance height, m
h_{ref} : Arbitrary standard thickness, m
H_r : Oil film thickness to surface roughness ratio, -
$\overline{h}_T$: Average oil film thickness, m
N : Orbital speed, rpm
p : Oil film pressure, Pa
p_a : Atmospheric pressure, Pa
p_c : Plastic flow pressure, Pa
p_{in}, p_{out} : boundary pressure, Pa
r_i, r_o : Inner bearing radius, m
$\overline{U}$, $\overline{W}$: Non-dimensional average oil flow velocity, -
$\overline{u}$, $\overline{w}$: Average oil flow velocity, m/s

U_l, V, W_l : Boundary velocity, m/s
V_{r1}, V_{r2} : Variance ratio, -
α : Wedge angle, rad
α^* : **Local solid contact ratio, -**
β : Asperity summits radius, **m**
Δp : Pressure difference, Pa
η : Surface density of asperities, m^{-2}
Θ : Orbiting angle, rad
λ : Bearing number, -
λ^* : Non-dimensional factor for oil flow velocity, -
μ : Coefficient of friction, -
μ^* : Oil viscosity, $Pa \cdot s$
$\sigma, \sigma_1, \sigma_2$: Standard deviations of surface combined roughness, m
$\overline{\sigma}$: Non-dimensional deviations of surface combined roughness, -
σ_s : Squeeze number, -
τ_t : Non-dimensional time, rad
τ : Shearing strength, Pa
ϕ : Pressure flow factor, -
ϕ_s : Shear flow factor, -
ϕ_f, ϕ_{fs} : Shear stress factor, -
ψ_x, ψ_y : Rotation angle rotating x - axis, rad
ω : Angular orbiting velocity, rad/s

REFERENCES

1. Ishii, N., Oku, T., Anami, K., Fukuda, A., 2004, Lubrication Mechanism at Thrust Slide-bearing of Scroll Compressors (Experimental study), *Proc. of 17th Int. Comp. Engrg. Conf. at Purdue*, C103, pp. 1-8.
2. Ishii, N., Oku, T., Yoshihiro, N., Matsui, A., Anami, K., C. W. Knisely., Sawai, K., Morimoto, T., Iida, N., 2007, A study on the lubrication mechanism at thrust slide-bearing of scroll compressors, *Proc. of International Conference on Compressors and their Systems*, pp. 513- 524.
3. Ishii, N., Oku, T., Anami, K., Knisely, C.W., Sawai, K., Morimoto, T., Iida, N., 2008, Experimental Study of the Lubrication Mechanism for Thrust Slide Bearings in Scroll Compressors, HVAC&R Research Journal ASHRAE Vol.14, No.3, pp. 453-465.
4. Oku, T., Anami, K., Ishii, N., Sano, K., 2004, Lubrication mechanism at thrust slide-bearing of scroll Compressors (Theoretical study), *Proc. of 17th Int. Comp. Engrg. Conf. at Purdue*, C104, pp. 1-8.
5. Oku, T., Ishii, N., Anami, K., Knisely, C.W., Sawai, K., Morimoto, T., Hiwata, A., 2008, Theoretical Model of Lubrication Mechanism in the Thrust Slide-Bearing of Scroll Compressors, *HVAC&R Research Journal* ASHRAE Vol.14, No.2, pp. 239-258.
6. Oku, T., Anami, K., Ishii, N., Charles W. K., Sawai, K., Morimoto, T., Hiwata, A., 2006, Optimal Performance Design Method of Thrust Slide-Bearing in Scroll Compressors for Its Best Efficiency, *Proc. of 18th Int. Comp. Engrg. Conf. at Purdue*, C128, pp. 1-8.
7. Ishii, N., Oku, T., Anami, K., Knisely, C.W., Sawai, K., Morimoto, T., Iida, N., 2008, Optimal Performance Design Guidelines of Thrust Slide-Bearing in Scroll Compressors for Maximum Efficiency, *Proc. of Int. Comp. Engrg. Conf. at Purdue*, 1428, pp. 1-8.
8. Patir, N. & Cheng, H. S., 1978, An average flow model for determining effects of three dimensional roughness on partial hydrodynamic lubrication, *Transactions of the ASME* , Vol. 100, pp. 12-17.
9. Patir, N. & Cheng, H. S., 1979, Application of average flow model to lubrication between rough sliding surfaces, *Transactions of the ASME* , Vol. 101, pp. 220-230.
10. Greenwood, J.A. & Williamson, J.B.P., 1966, Contact of nominally flat surfaces, Burndy Corporation Research Division, Norwalk, Connecticut, USA, pp. 330-319.

ACKNOWLEDGEMENT